Technical University of Denmark

DTU

A phase-field simulation study of irregular grain boundary migration during recrystallization

Moelans, N.; Zhang, Yubin; Godfrey, A.; Juul Jensen, Dorte

Link back to DTU Orbit

DTU Library
Technical Information Center of Denmark

A phase-field simulation study of irregular grain boundary migration during recrystallization

N Moelans[1], Y B Zhang[2], A Godfrey[3], D Juul Jensen[2]

[1]Department of Materials Engineering, KU Leuven, Kasteelpark Arenberg 44, Box 2450,
B-3001 Leuven, Belgium
[2]Danish Chinese Center for Nanometals, Section for Materials Science and Advanced
Characterization, Department of Wind Energy, Risø Campus, Technical University of
Denmark, DK-4000 Roskilde, Denmark
[3]Key Laboratory of Advanced Materials (MOE), School of Materials Science and Engineering,
Tsinghua University, Beijing 100084, Peoples Republic of China

E-mail: `nele.moelans@mtm.kuleuven.be`

Abstract. We present simulation results based on a phase-field model that describes the migration of recrystallization boundaries into spatially varying deformation energy fields. Energy fields with 2-dimensional variations representing 2 sets of dislocation boundaries lying at equal, but opposite, angles to the moving boundary are considered. The simulations show that the shape and overall migration rate of the recrystallization front is considerably affected by spatial variations in the deformation microstructure. It is seen that, depending on characteristics of the variations in the deformation microstructure, highly asymmetrical protrusions and retrusions can develop on the migrating recrystallization front resulting in a migration velocity considerably larger than that expected from standard recrystallization models. It is also seen that, when the wavelength of the variations in a deformation microstructure along the grain boundary is larger than the wavelength of the variations in the direction of migration, parts of the boundary show a stop-and-go type of migration, resulting in a lower overall migration rate. These simulations thus reproduce and explain many of the typical features observed in recrystallization experiments. They give new insights in the way deformation microstructures can affect the migration behavior of recrystallization boundaries and can lead to a stop-and-go type of migration of the recrystallization boundary even in pure materials.

1. Introduction
During recrystallization new almost defect free grains grow in a deformed matrix containing dislocations and other defects. In recrystallization studies, it is generally assumed that the driving force for recrystallization is homogeneous along the recrystallization boundary and that the boundary moves smoothly with a velocity v_{gb} proportional to the (homogeneous) driving force for recrystallization P_{rex}:

$$v_{gb} = MP_{rex}, \tag{1}$$

where M is called grain boundary mobility. Extensive studies [1] have however shown that local variations exist in the deformed microstructures and that grain boundary movement during recrystallization is often very irregular, even in pure materials [2–6].

For instance, the arrangement of the dislocations within a deformed grain typically shows significant local variations. Often dislocations organize themselves into boundaries in the form of

a cell block microstructure, where dislocation boundaries of larger misorientation angles delineate volumes containing interconnecting dislocation boundaries of smaller misorientation [7–9]. Local variations in the spacing between and misorientation angle across the dislocation boundaries are generally observed. The driving force for recrystallization can consequently vary significantly even along a short length of a recrystallization boundary.

In-situ experiments of the movement of a recrystallization boundary have indeed shown that individual grain boundary segments move with different rates [2, 3, 5]. For example, in-situ observations and ex-situ microstructural studies of recrystallization in materials with medium to high stacking fault energy, such as Ni and Al, clearly show the presence of protrusions (parts of the boundary that have advanced more than other parts) and retrusions (parts of the boundary that are behind) of a few up to tens of μm along recrystallization boundaries. Moreover the boundary profile is dynamic: protrusions can disappear or transform into retrusions and vice-versa as a migrating recrystallization boundary moves into a deformed matrix. Often parts of the boundary also show a stop-and-go type of movement.

Zhang et al. [10, 11] have measured the curvatures at protrusions and retrusions formed along recrystallization boundaries and related these values to the local stored deformation energy in front of the moving boundary. It appeared that the magnitude of the local curvature based driving force for grain boundary migration at protrusions and retrusions is comparable to that of the stored energy within the deformed microstructure and thus cannot be neglected when characterizing the local migration rate of a recrystallization boundary. Although, large variations in stored deformation energy may result in protrusions and retrusions with high curvatures, the size and shape of the protrusions and retrusions seem to be correlated in a complex way to the spatial variations in the stored deformation energy [10].

Recently, we presented an approach based on a phase-field model to simulate the formation of protrusions and retrusions during migration of a recrystallization boundary into a deformation microstructure containing variations in stored energy [12]. The deformation energy field for the model is assumed to be constant in time and constructed to represent characteristics of typical deformation microstuctures obtained for medium-to-large strains.

As the simplest model to capture the typical variations in stored energy in a deformation microstructure, we considered energy fields with 1-dimensional variations representing a single set of dislocation boundaries. One dimensional functions with maxima at the positions of the cell block boundaries and minimum energy in the cell block interior were considered.

The model was able to reproduce the experimentally observed asymmetry between the protrusion and retrusion curvatures. Furthermore, we found that the characteristics of the spatial variations in stored deformation energy density have strong effects on the shape of the boundary and, more importantly, the overall boundary migration rate. For variations with low amplitude or small wavelength, the protrusions and retrusions are almost symmetric and the overall boundary velocity scales with the average stored deformation energy density, in agreement with generally accepted theories of recrystallization (assuming a homogeneous driving force along the recrystallization boundary). For large amplitudes and/or large wavelengths of the variations, an asymmetrical grain boundary shape is obtained with much larger curvatures at the retrusions than at the protrusions. In this case, the velocity scales with the maximum of the deformation energy density along the variation, resulting in a considerably larger velocity than that obtained assuming that the same energy would be distributed homogeneously in the material. The net driving forces due to curvature obtained in the simulations are similar in magnitude to those calculated from experimental micrographs.

The model can however easily treat more complex variations in stored deformation energy. Our long term aim is a systematic study of the effect of different characteristics of the spatial variations in deformation energy on the shape and velocity of a migrating recrystallization boundary, considering gradually more and more complex energy distributions.

In this paper, a more complex, but still idealized, case is considered, namely the migration into deformation energy fields with 2-dimensional variations representing dislocation boundaries in 2 directions. The simulation results are discussed and the findings are compared with those from the simulations with 1-dimensional variations.

2. Simulation details

We refer to our previous paper [12] for a detailed description of the phase-field model used for the simulations. The spatial variations in stored deformation energy are assumed to be constant in time (i.e. no recovery is included in the simulations) and are included in the model description using a free energy density term $f_{def}(x, y)$, which is a function of the spatial coordinates and can be of any continuous or discontinuous form that describes the deformation field.

In the present study, the movement of an initially planar boundary into energy fields with 2-dimensional variations representing 2 sets of dislocation boundaries lying at equal, but opposite angles to the boundary are considered. The considered deformation energy fields are shown in figures 1a and 2a using a color scaling, with black representing the highest energy density and white an energy density equal to 0. They are constructed as follows

$$f_{def}(x, y) = \max(f_{def,1}(x, y), f_{def,2}(x, y)) \tag{2}$$

with

$$f_{def,1}(x, y) = A_{def} \left[1 + \sin\left(\frac{\lambda_{def}}{|\sin(\alpha)|} \left(x - \frac{y}{\tan(\alpha)} \right) \right) \right] \tag{3}$$

$$f_{def,2}(x, y) = A_{def} \left[1 + \sin\left(\frac{\lambda_{def}}{|\sin(\alpha)|} \left(x - \frac{y}{\tan(-\alpha)} \right) \right) \right] \tag{4}$$

with α and $-\alpha$ the angles between the x-axis and the orientations of the 2 sets of dislocation boundaries, λ_{def} the spacing between the dislocation boundaries (i.e. the wavelengths of the variations measured perpendicular to the dislocation boundaries) and A_{def} the amplitude of the variations. The movement of initially flat grain boundaries in either the x- or y-direction into these fields is simulated.

In our previous study considering 1-dimensional variations, values for A_{def}, λ_{def} and the grain boundary energy σ_{gb} were chosen based on experimental information [9–11, 13] for aluminium and nickel: the amplitude of the variations A_{def} was varied between 0.1 and 20 MJ/m^3, the wavelength λ_{def} was taken 1.6, 3.2 and 6.4 μm for the symmetrical variations and the grain boundary energies of $\sigma_{gb} = 0.32$ J/m^2 (aluminium) and $\sigma_{gb} = 0.87$ J/m^2 (nickel) were used. The remaining model and simulation parameters were taken based on numerical considerations, such that grain boundary motion is resolved with a numerical error smaller than 5 % [14–16].

Similar parameter values are used in this work. Two energy fields are considered with $A_{def} = 1.3416$ MJ/m^3 and $\alpha = \pi/12$ and for one field $\lambda_{def} = 1.66$ μm and for the other field $\lambda_{def} = 6.18$ μm. The average deformation energy present in the material is then $f_{def,av} = 1.8850$ MJ/m^3 for both fields. One simulation was also performed assuming a grain boundary migrating into a homogeneous deformation energy field with energy density $f_{def} = f_{def,av} = 1.8850$ MJ/m^3. A grid spacing of $\Delta x = 0.05$ μm and time step of $\Delta t = 0.1$ s were used. The grain boundary mobility was arbitrarily taken as $M = 1.7 \times 10^{-15}$ m^4/(Js), since experimental values for the grain boundary mobility are hard to find and strongly dependent on solute content. The value of M however only affects the time scaling of the simulations.

3. Simulation results

The images in figure 1 show the boundary positions obtained every 1000 time steps in the simulations (Starting from time step 40000 to be in the regime where the grain boundary
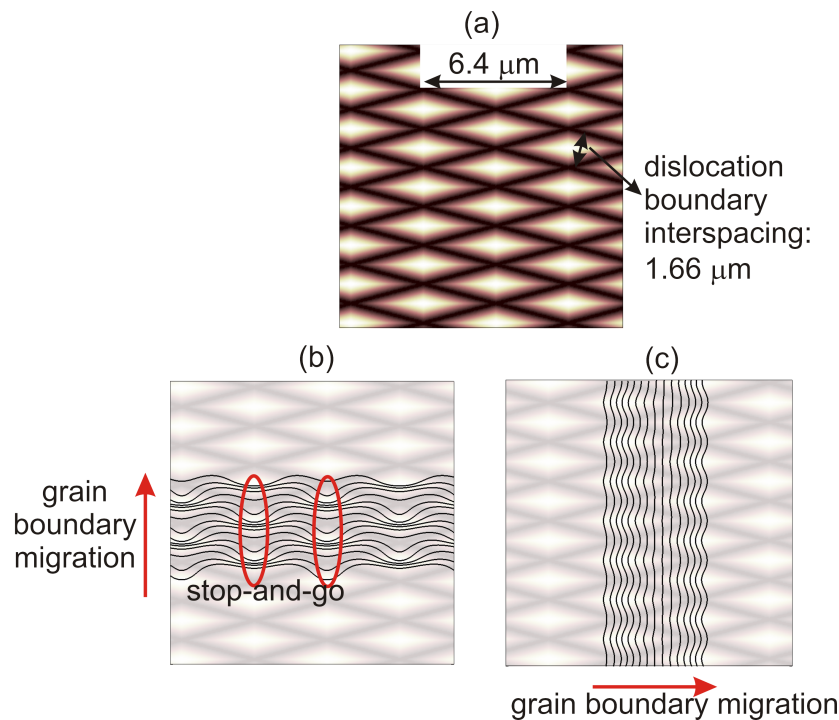
Figure 1. Simulation results obtained for a recrystallization boundary migrating in a deformation energy field with variations given by equations (2)-(4) with $A_{def} = 1.3416$ MJ/m^3, $\alpha = \pi/12$ and $\lambda_{def} = 1.66\mu$m. (a) Representation of the considered energy field using a color scaling with black representing the highest energy density and white an energy density equal to 0. (b), (c) Grain boundary positions as a function of time obtained in the simulations, plotted every 1000 time steps starting from time step 40000. (b) Boundary moving from bottom to top. Parts of the boundary, indicated with the red ovals, show a stop-and-go type movement: boundary parts near minima in the energy density field remain for a longer period at the same position and then advance suddenly to the next minimum in the energy density. (c) Boundary moving from left to right. Almost symmetrical protrusions and retrusions develop along the migrating recrystallization front. Protrusions transform into retrusions and vice-versa in a continuous way while the grain boundary is migrating, due to the spatial variations in deformation energy density. (a), (b) and (c): Only part of the simulation domain is shown.

shape varies periodically in time. The initial migration behavior starting from a flat boundary will be analysed in later work) for the 2-dimensional field described by equations (2)-(4) with $A_{def} = 1.3416$ MJ/m^3, $\alpha = \pi/12$ and $\lambda_{def} = 1.66\mu$m, considering the migration of a recrystallization boundary in the y- (figure 1a) and x-direction (figure 1b) of the simulation domain. Protrusions and retrusions clearly form along the migrating recrystallization boundary. The migration behavior in the y-direction (from bottom to top) is very different from that in the x-direction (from left to right). For the boundary migrating in the y-direction, parts of the grain boundary located near a minimum in the energy field (where the energy density is almost 0) almost stop moving for some time and then advance quickly to the next position with minimum energy density, very similar to the stop-and-go behavior seen in experiments. The movement of the boundary migrating in the x-direction, on the other hand, is smooth. Protrusions and retrusions develop symmetrically with a shape that is very similar to the protrusion/retrusion shapes seen in the simulations with 1-dimensional variations with small
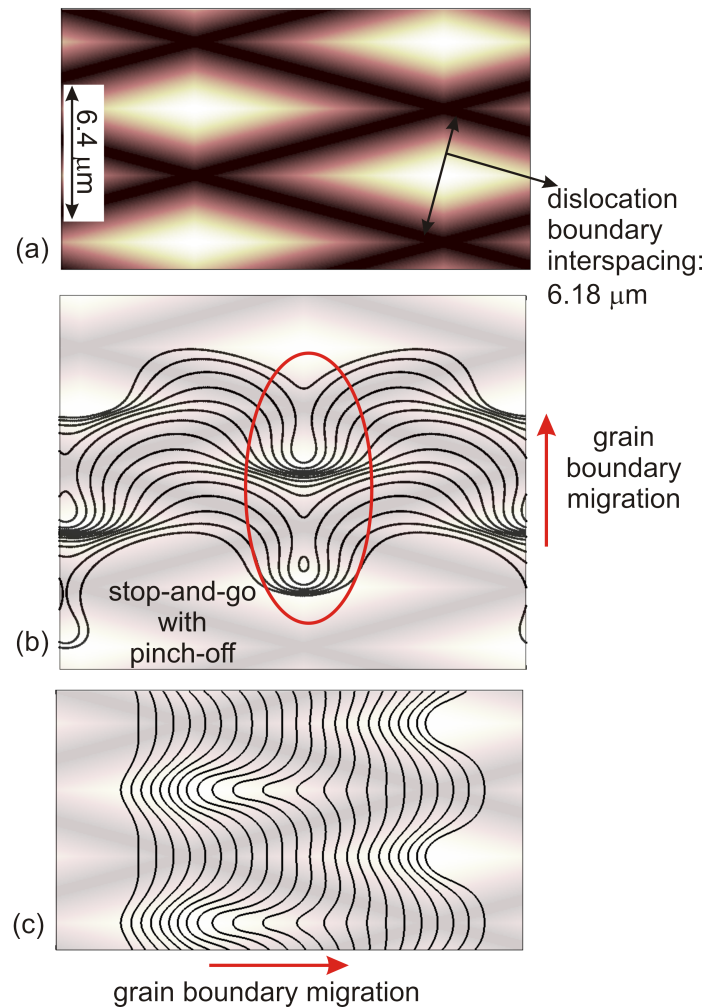
Figure 2. Simulation results obtained for a recrystallization boundary migrating in a deformation energy field with variations given by equations (2)-(4) with $A_{def} = 1.3416$ MJ/m^3, $\alpha = \pi/12$ and $\lambda_{def} = 6.18\mu$m. (a) Representation of the considered energy field using a color scaling with black representing the highest energy density and white an energy density equal to 0. (b), (c) Grain boundary positions as a function of time obtained in the simulations, plotted every 2000 time steps starting from time step 60000. (b) Boundary moving from bottom to top. Parts of the boundary, indicated with the red oval, show a stop-and-go type of movement with pinch-off: boundary parts near minima in the energy density field remain for a longer period at the same position, while the rest of the boundary continues to advance. At a certain point, the stagnated parts are pinched off, leaving behind a small part of deformed material. (c) Boundary moving from left to right. Asymmetrical protrusions and retrusions develop along the migrating recrystallization front with a considerably higher curvature at the retrusions than at the protrusions. Protrusions transform into retrusions and vice-versa in a continuous way while the grain boundary is migrating. (a), (b) and (c): Only part of the simulation domain is shown.

wavelength. Different, however, from the simulations with 1-dimensional variations, no steady-state is reached. Protrusions transform into retrusions and vice-versa during grain boundary migration due to the variations in stored deformation energy experienced by the boundary.

The boundary positions obtained every 2000 time steps in the simulations (starting from time
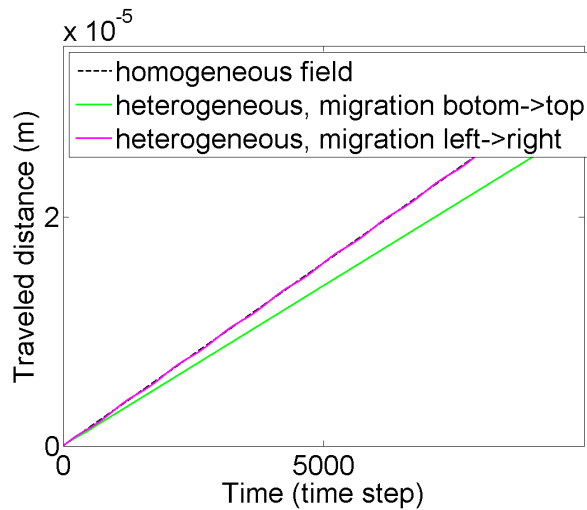
Figure 3. Average travel distance as a function of time obtained for recrystallization boundaries migrating into a varying energy field given by equations (2)-(4) with $A_{def} = 1.3416$ MJ/m^3, $\alpha = \pi/12$ and $\lambda_{def} = 1.66$ μm, in either the y- (bottom to top) or x-direction (left to right). The travel distance of a recrystallization boundary migrating in a homogeneous energy field with the same average energy density is also shown for comparison.

step 60000) with a 2-dimensional energy field described by equations (2)-(4) with $A_{def} = 1.3416$ MJ/m^3, $\alpha = \pi/12$ and $\lambda_{def} = 6.18\mu$m, are shown in figure 2. Again protrusions and retrusions clearly develop on the migrating recrystallization boundaries. For the boundary migrating in the y-direction, parts of the boundary located near a minimum in the stored deformation energy field stagnate and are pinched off from the boundary after some time. Because of the larger spacings between the dislocation boundaries, the moving parts of the boundary can bow out so widely that the parts of the moving grain boundary on both sides of the stagnated part can join and pinch off a part of the boundary, leaving behind an island of unrecrystallized material. The boundary migrating in the x-direction migrates smoothly. For this field, asymmetrical protrusions and retrusions with a much higher curvature at the retrusions than at the protrusions form along the boundary. Periodically, protrusions transform into retrusions and vice-versa.

Comparison of figures 1 and 2 shows that for one given value of the amplitude in the variations A_{def}, boundary movement becomes more irregular and the protrusions and retrusions become more asymmetric for increasing distance between the dislocation boundaries λ_{def}. The increasing asymmetry between the protrusion and retrusion curvature with increasing wavelength of the variations is consistent with our findings from the simulations with 1-dimensional variations. The stagnation of parts of the grain boundary at positions where the stored deformation energy is close to 0, was not observed in the simulations with 1-dimensional variations. From the considered cases, we conclude that stagnation of parts of the grain boundary occurs when the wavelength of the spatial variations along the grain boundary is larger than that of the variations in the direction of the movement. In contrast, when the wavelength of the variations in the direction of movement is larger than that of the variations along the grain boundary, the energy variations experienced by the grain boundary look similar to a 1-dimensional variation over a considerable distance and therefore protrusions and retrusions, with a shape very similar to those seen in the simulations with 1-dimensional variations, can develop.

Figure 3 gives the average distance travelled as a function of time of the migrating recrystallization boundaries considered in figure 1 ($\lambda_{def} = 1.66\mu$m). The graphs show that for this small distance between the dislocation boundaries and medium stored deformation energy, the stop-and-go behavior observed for parts of the boundary when migrating in the y-direction of the simulation domain, results in a smaller travelled distance at each time than expected (green curve) than expected from equation (1) with $P_{rex} = f_{def,av}$ used in classical recrystallization studies. For the boundary migrating in the x-direction, the curvatures at the protrusions and retrusions remain almost symmetric. Consistent with observations in the simulations with 1-
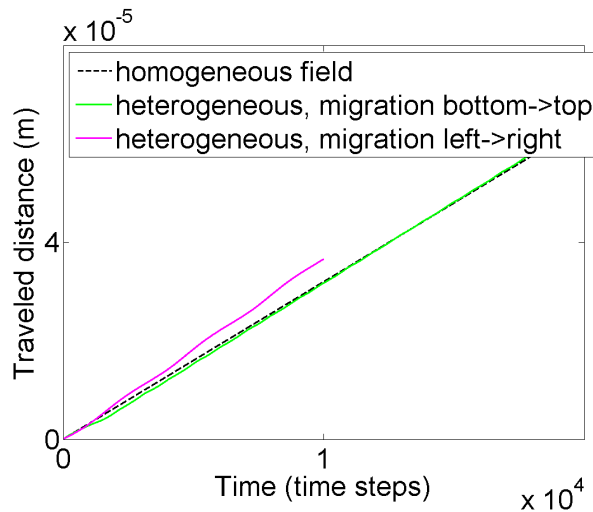
Figure 4. Average travel distance as a function of time obtained for recrystallization boundaries migrating into a varying energy field given by equations (2)-(4) with A_{def} = 1.3416 MJ/m^3, α = $\pi/12$ and λ_{def} = 6.18 μm, in either the y- (bottom to top) or x-direction (left to right). The travel distance of a recrystallization boundary migrating in a homogeneous energy field with the same average energy density is also shown for comparison.

dimensional variations, the average displacement (magenta curve) then equals that of a boundary migrating in a homogeneous deformation energy field with the same average energy density, except for a small periodic variation in velocity, resulting from the continuous transformation of protrusions into retrusions and vice-versa.

Figure 4 gives the average travel distance as a function of time for the recrystallization boundaries considered in figure 2 (λ_{def} = 6.18μm). For this stored deformation energy field, the average displacement (green curve) of the grain boundary migrating in the y-direction as a function of time is close to that obtained for a recrystallization boundary moving in a homogeneous field with the same average energy density, although parts of this boundary show a stop-and-go type of migration. Because of the wider spacing in between the dislocation boundaries, the moving parts of the boundary can still advance considerably when other parts of the boundary are pinned. Moreover, the moving parts of the grain boundary can bow out sufficiently to pinch off the stagnated boundary parts, reducing the effect of the stagnation of these parts on the average grain boundary velocity. For the considered conditions, the resulting grain boundary velocity appears to be close to that observed for a homogeneous field with the same average energy density. It would be interesting, however, to study in detail as a function of the amplitude of the variations and the distance between dislocation boundaries how the stop-and-go type of movement of parts of a recrystallization boundary affect its average velocity. This will be done in a future investigation. On the boundary migrating in the x-direction, protrusions and retrusions with a considerably larger curvature at the retrusions develop. Consistent with the findings from our previous simulations with 1-dimensional variations, a larger average velocity (magenta curve) is obtained in this case compared to the case of a boundary migrating into a homogeneous deformation field with the same average energy density. The grain boundary velocity is thus considerably larger than that expected from standard recrystallization models. Since the curvatures at the retrusions result in an extra driving force in the direction of grain boundary migration, this higher velocity can be explained by the higher curvature at the retrusion tips than at the protrusion tips, resulting in a net curvature driving force in the direction of grain boundary migration. As the size of the protrusions and retrusions varies periodically in time, there is a small perodic variation in the velocity with time.

4. Conclusions
A previously developed phase-field model has been applied to study the migration behavior of recrystallization boundaries into deformation energy fields with 2-dimensional variations,

representing 2 sets of dislocation boundaries, lying at equal, but opposite, angles to the moving recrystallization front. Compared to the results from previous simulations with 1-dimensional variations, more complex migration behavior, very similar to that observed in experiments, is obtained in these simulations. Nevertheless the conclusions from the simulations with 1-dimensional variations are still relevant.

The simulations show that the deformation microstructure and the orientation of the recrystallization boundary have a large effect on the shape and overall velocity of the migrating boundary. Although the grain boundary properties were chosen to be isotropic, very different migration behavior was obtained for migration in the x- and y-direction of the simulation system for the same deformation energy field. When the wavelength of the variations perpendicular to the grain boundary is larger than that of the variations along the boundary, smooth migration of the recrystallization boundary is observed with the development of protrusions and retrusions along the grain boundary. The protrusion/restrusion shapes are in this case very similar to those observed in the simulations with 1-dimensional variations. For a large enough distance between the dislocation boundaries, the curvatures obtained at the retrusions are much larger than those obtained at the protrusions, resulting in an average grain boundary displacement considerably larger than that obtained for a grain boundary moving in a homogeneous field with equal average stored deformation energy density. When the wavelength of the variations perpendicular to the grain boundary is smaller than that of the variations along the boundary, parts of the boundary undergo a stop-and-go type of movement. Moreover, if the distance between the dislocation boundaries is large enough, the stagnated parts of the recrystallization boundary can pinch off, leaving behind a small domain of unrecrystallized material. The stop-and-go type of movement of parts of the boundary generally results in a lower average grain boundary velocity.

These insights highlight the need for reliable experimental data on stored deformation energy on the scale of the local heterogeneities in deformation microstructures. The simulation results also motivate a detailed quantitative study of the effect of characteristics of 2-dimensional variations in stored deformation energy density on the shape and migration velocity of recrystallization boundaries.

References
[1] Hansen N and Juul Jensen D 2011 *Materials Science and Technology* **27** 1229–1240
[2] Beck P and Sperry P 1950 *J. Appl. Phys.* **21** 150
[3] Schmidt S, Nielsen S F, Gundlach C, Margulies L, Huang X and Juul Jensen D 2004 *Science* **305** 229–232
[4] Xu W, Quadir M Z and Ferry M 2009 *Metall. Mater. Trans. A* **40A** 1547–1556
[5] Zhang Y B, Godfrey A, Liu Q, Liu W and Juul Jensen D 2009 *Acta Mater.* **57** 2631–2639
[6] Martorano M A, Sandim H R Z, Fortes M A and Padilha A F 2007 *Scripta Mater.* **56** 903–906
[7] Godfrey A, Juul Jensen D and Hansen N 1998 *Acta Mater.* **46** 823–833
[8] Godfrey A, Juul Jensen D and Hansen N 1998 *Acta Mater.* **46** 835–848
[9] Godfrey A, Hansen N and Juul Jensen D 2007 *Metall. Mater. Trans. A* **38A** 2329–2339
[10] Zhang Y B, Godfrey A and Juul Jensen D 2009 *CMC-Computers Materials & Continua* **14** 197–207
[11] Zhang Y B, Godfrey A and Juul Jensen D 2011 *Scripta Mater.* **64** 331–334
[12] Moelans N, Godfrey A, Zhang Y B and Juul Jensen D 2013 *Phys Rev B* **88** 054103
[13] Knudsen T, Cao W Q, Godfrey A, Liu Q and Hansen N 2008 *Metall. Mater. Trans. A* **39A** 430–440
[14] Moelans N, Blanpain B and Wollants P 2008 *Phys. Rev. B* **78** 024113
[15] Moelans N, Wendler F and Nestler B 2009 *Comp. Mater. Sci.* **46** 479–490
[16] Moelans N 2011 *Acta Mater.* **59** 1077–1086